



Polyethylene microplastics as adsorbent of diazinon in aqueous environments: optimization, and modeling, isotherm, kinetics, and thermodynamic studies

Mohammadreza Yari^{1,2} · Ziaeddin Bonyadi² · Aliasghar Najafpoor² · Behnam Barikbin²

Received: 3 March 2024 / Accepted: 23 May 2024 / Published online: 5 June 2024
© The Author(s) 2024

Abstract

MPs have raised significant public concern due to their role as carriers of organic contaminants in aqueous solutions. DZN is a non-systemic organophosphorus pesticide that poses risks to human and environmental health. This study aimed to investigate the adsorption of DZN onto PE MPs by examining factors such as PE dose, reaction time, pesticide concentration, and pH through experimental runs based on the Box–Behnken model. According to the Langmuir model, the maximum adsorption capacity of PE for DZN was 0.35 mg/g. The results indicated that the highest adsorption rate of DZN (92%) was observed in distilled water, while the lowest adsorption rate (57%) was observed in municipal wastewater. The ΔH° and ΔS° values were obtained as -0.16 kJ/mol and 54.41 J/(mol K), respectively. Therefore, regarding negative ΔG° values, it can be concluded that the adsorption of DZN onto PE MPs is an exothermic, highly disordered, and spontaneous process. The findings indicate a reduction in the adsorption rate of DZN as the concentrations of interfering compounds increase. These findings offer understanding of the interaction between MPs and organic contaminants, emphasizing the need for further studies and approaches to reduce their harmful impact on human health and the environment.

Keywords Diazinon · Polyethylene · Microplastic · Pesticide

Abbreviations

MPs	Microplastics
DZN	Diazinon
PE	Polyethylene
EDX	Energy-dispersive X-ray spectroscopy
FTIR	Fourier transform infrared spectroscopy
FESEM	Field emission scanning electron microscopy
HPLC	High-performance liquid chromatography

ZP	Zeta potential
DLS	Dynamic light scattering

Introduction

Plastics are commonly used in our everyday lives because of their unique characteristics like being affordable, light-weight, strong, and long-lasting. The global production and consumption of plastic have increased significantly over the years, with plastic particles being found in marine ecosystems since the 1970s (Zahmatkesh Anbarani et al. 2023a, b). Plastic waste pollution is visible in various water bodies and sewage treatment plants, and it is estimated that by 2025, around 11 billion tons of plastic waste will have accumulated in the environment (Barari and Bonyadi 2023). Soil pollution caused by solid plastic waste poses a significant environmental threat (Wang et al. 2023a, b).

Larger plastic items can break down into smaller particles called MPs through natural processes like wear and exposure to sunlight. These particles are also present in cosmetic and industrial products (Esmaeili Nasrabadi et al. 2023). MPs are synthetic polymer particles or fibers with sizes ranging from

✉ Ziaeddin Bonyadi
Zyabonyadi@yahoo.com
Mohammadreza Yari
mry2246mry@gmail.com
Aliasghar Najafpoor
Najafpooraa@mums.ac.ir
Behnam Barikbin
Barikbinb@mums.ac.ir

¹ Student Research Committee, Mashhad University of Medical Sciences, Mashhad, Iran

² Department of Environmental Health Engineering, School of Health, Mashhad University of Medical Sciences, Mashhad, Iran

0.1 to 5000 μm , and their concentration in water bodies and shorelines can be quite high (Nasrabadi et al. 2023). Each year, approximately 300 million tons of MPs enter the environment, mostly in soil and freshwater environments (Zhang et al. 2021; Zahmatkesh Anbarani et al. 2024). MPs have a small size, large surface area, and high hydrophobicity, making them ideal carriers for various pollutants like pesticides, PCBs, cyanide, PAHs, Antibiotics, and heavy metals, which can easily spread throughout the ecosystem (Bonyadi et al. 2012; Esmaili et al. 2023; Yu et al. 2024). Feng et al. (2021) conducted a study examining the adsorption characteristics of three pesticides, including imidacloprid, buprofezin, and difenoconazole on PE MPs in a water-based solution (Li et al. 2021). The research highlighted the gradual adsorption of pesticides onto plastic layers utilized as protective covers in agricultural soil (Cheng et al. 2023). The geopolymers in the soil can be fragmented and destroyed in a complex process under the influence of environmental factors such as temperature, humidity, and microbial activity, turning into microplastic particles (Bai et al. 2023). The proximity of agricultural PE MPs to human habitats compared to marine microplastics results in a more severe combined pollution of plastic and pesticides in soil, posing increased risks to human health (Lan et al. 2021; Eydi Gabrabad et al. 2024). Studies indicate a significantly higher abundance of these pollutants in terrestrial environments, ranging from 4 to 23 times more prevalent than in marine settings (Beg et al. 2016; Zhou et al. 2024). Even red mud in agricultural soil can interact with PE mulch and DZN, affecting their degradation and persistence in the environment (Chen et al. 2024). PE, a versatile material widely employed in agriculture, composite materials, and packaging, is a predominant component of microplastics found in various water bodies. It has been reported that mulch layers made of plastic contain significant amounts of pesticides, with concentrations ranging from 584 to 2284 mg/g (Salama and Geyer 2023). Agricultural soil contamination by pollutants such as heavy metals, pesticides, and toxic organic chemicals poses significant risks to both human health and the environment (Foroutan et al. 2020; Zafarzadeh et al. 2021). It is estimated that 12.5 million tons of plastic products are used annually for agricultural purposes. In some parts of the world, plastics used in agriculture absorb environmental pollutants, such as toxins (Mongil-Manso et al. 2023). Previous studies have demonstrated the adsorption of pesticides, such as diflufenuron and difenoconazole, onto PE MPs. Additionally, the presence of MPs in water has been linked to a reduction in pesticide residues (Wang et al. 2020a, b). PE MPs can infiltrate water environments and may pass through water treatment plants untreated, ultimately entering the drinking water distribution network (Du et al. 2022).

Pesticides are transferred to other environments through MPs. Due to their relatively high resistance to degradation

by environmental factors, MPs enter the food chain, posing a threat to both humans and the environment (Pirsaheb et al. 2013; Kafaei et al. 2020). DZN, a non-systemic organophosphorus pesticide, is known for its moderate water solubility and resistance (Ehrampoush et al. 2017). DZN poses significant health risks due to its inhibitory effects on enzymes, particularly acetylcholinesterase, leading to central nervous system disorders and a range of adverse effects, including gastrointestinal, neurological, mutagenic, and carcinogenic manifestations. Symptoms of DZN poisoning include intestinal contractions, chest tightness, blurred vision, headaches, diarrhea, hypotension, coma, and various neurological complications (Haji Abolhasani and Sahebghadam Lotfi 2022).

This article investigated the impact of PE MPs on the adsorption of DZN pesticide in aquatic environments, aiming to provide a more comprehensive understanding of the potential ecological consequences. The study aims to investigate the impact of PE on the adsorption of DZN pesticide in aquatic solutions, focusing on how PE influences the adsorption process and the distribution of DZN pesticide in water bodies. Additionally, the study seeks to characterize the properties of PE using EDX, FTIR, and FESEM to analyze the elemental composition, functional groups, and surface morphology of PE.

Materials and methods

Materials

PE granules, characterized by a high purity percentage, white color, and transparency, were acquired from an engineering company in Mashhad, Iran, and processed into MPs of various dimensions using a mechanical milling technique. DZN was acquired from the Sigma-Aldrich company with a purity of 99%. Other chemicals with a purity of 99%, such as CaCO_3 , MgSO_4 , NaHCO_3 , NaNO_3 , Na_2HPO_4 , NaCl , HCl , NaOH , methanol, and distilled water of HPLC grade, were obtained from Merck Company (Germany).

MPs preparation

Initially, PE MPs were pulverized using a grinder and sifted into sizes less than 425 μm . Subsequently, to eliminate organic compounds from the surfaces of MPs, they were immersed in an ethanol solution for 48 h with agitation using a magnetic stirrer, rinsed with distilled water, and desiccated in an oven at 50 °C. A DZN solution was prepared at an initial concentration of 30 mg/L. Then, a series of DZN solutions were prepared at concentrations ranging from 0.5 to 8.5 mg/L and stored in a shaded and cool environment.

Preparation of reaction mixture

The reaction mixture, comprising 50 cc, was exposed to different conditions, such as the initial DZN concentration (ranging from 0.5 to 8.5 mg/L), solution pH (ranging from 4 to 10), adsorbent dose (ranging from 0.2 to 1 g/L), and reaction time (ranging from 10 to 90 min). Table 1 outlines the scope and levels of the key factors used for DZN adsorption.

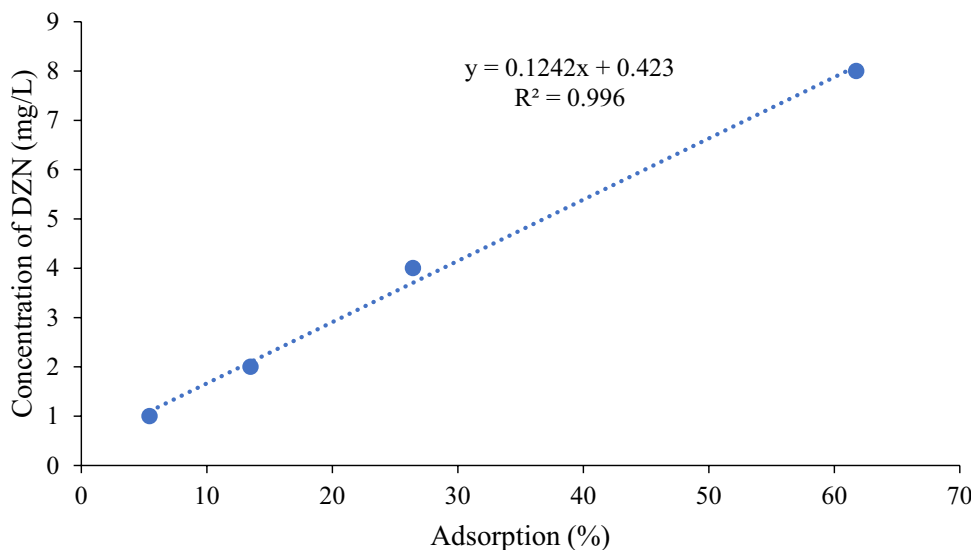
Analytical methods

At defined time intervals, 10 mL of sample was extracted from each Erlenmeyer flask. Subsequently, the samples were centrifuged at 4000 rpm for 10 min. The concentration of DZN was determined using an HPLC (KNAUER model, Germany) at a wavelength of 275 nm and a flow rate of 1 mL/min. The analysis was performed on a C-18 column that was 25 cm in length and 6.4 mm in diameter, at ambient temperature, using a mobile phase consisting of a methanol-to-water ratio of 30:70 (Ehrampoush et al. 2017). The adsorption rate of DZN was determined using formula 1:

Table 1 Range and levels of the main factors used for DZN adsorption

Parameter	Code	Variable level		
		-1	0	+1
DZN Conc. (mg/L)	A	0.5	4.5	8.5
Time (min)	B	10	50	90
PE dose (g/L)	C	0.2	06	1
pH	D	4	7	10

Fig. 1 DZN calibration curve at concentrations ranging from 0.5 to 8.5 mg/L



$$\text{DZN adsorption}\% = \frac{(C_0 - C_e)}{C_0} \times 100 \tag{1}$$

where “ C_0 ” represents the initial level of DZN (mg/L) and “ C_e ” represents the equilibrium level of DZN (mg/L).

$$q_e = \frac{(C_0 - C_e)}{m} \times V \tag{2}$$

where “ m ” represents the mass of PE (g), and “ V ” represents the volume of the reaction mixture (L). Figure 1 shows DZN calibration curve at levels ranging from 0.5 to 8.5 mg/L.

Thermodynamic equation

In order to advance our comprehension of the adsorption mechanism of the DZN pesticide on polyethylene (PE), a thorough thermodynamic analysis was carried out. The tests of adsorption thermodynamics were conducted under various conditions, including PE MPs (0.6 g/L) and diazinon (0.5 mg/L), at different temperatures (288 °K, 298 °K, 308 °K, 318 °K) for a duration of 50 min at a pH of 10. The thermodynamic parameters, namely the standard enthalpy change (ΔH°) as per Eq. (3), standard entropy change (ΔS°) as per Eq. (4), and standard Gibbs free energy change (ΔG°) as per Eq. (5), were determined (Frescura et al. 2023):

$$\Delta G^\circ = -RT \ln K \tag{3}$$

$$\Delta G^\circ = \Delta H^\circ - T\Delta S^\circ \tag{4}$$

$$\ln K = -\frac{\Delta H^\circ}{RT} + \frac{\Delta S^\circ}{R} \tag{5}$$

In this formula, ΔG represents the change in Gibbs free energy measured in kJ/mol, K stands for the equilibrium

constant, R denotes the gas constant (8.314 J/mol K), and T signifies the temperature in °K (Bonyadi et al. 2022).

Results and discussion

Characterization

FT-IR

The FTIR spectrum of PE was shown in Fig. 2a and b before and after adsorbing DZN. In Fig. 1a, the peak at 3426.47 cm^{-1} is linked to O–H groups. Peaks at 2919.39 cm^{-1} and 2850.41 cm^{-1} represent the asymmetric and symmetric stretches of CH_2 , respectively. The peak at 1747.83 cm^{-1} corresponds to C=O stretching bands. The peak at 1468 cm^{-1} indicates bending deformation, while the peak at 1373 cm^{-1} corresponds to symmetric deformation of CH_3 . The peak at 719.29 cm^{-1} shows the presence of the benzene ring, which remained largely unchanged after removal. (Caro and Comas 2017). Figure 2b shows that the DZN pesticide most likely contains C–H and C–O groups. Figure 2b shows that the adsorption bands of the DZN pesticide underwent changes in vibration and intensity range after being adsorbed by PE. The FTIR spectrum of PE after DZN adsorption exhibits several characteristic peaks. The peak observed at 3437.44 cm^{-1} in the spectrum indicates the possible existence of hydroxyl groups or adsorbed water molecules. Peaks detected at 2918.65 cm^{-1} and 2850.45 cm^{-1} are associated with the stretching vibrations of C–H bonds in methylene (CH_2) groups inherent to PE. The presence of carbonyl groups (C=O) is suggested by the peak at

1747.83 cm^{-1} , potentially arising from chemical interactions between DZN and PE. The peak at 1630.43 cm^{-1} indicates unsaturation, which could be attributed to DZN or reactions with PE. Peaks at 1469.23 cm^{-1} , 1376.65 cm^{-1} , and 1306.53 cm^{-1} are linked to bending vibrations of methylene (CH_2) groups, confirming the presence of PE. The peak at 1155.25 cm^{-1} is associated with C–O stretching vibrations, indicating the formation of ether or ester groups during DZN adsorption. Furthermore, the peak at 1080.24 cm^{-1} corresponds to C–O–C stretching vibrations, providing additional evidence for the presence of ether groups. The peak at 719.23 cm^{-1} suggests the existence of aromatic C–H bending vibrations, potentially originating from DZN or its degradation byproducts. Lastly, the peak at 452.32 cm^{-1} corresponds to C–H bending vibrations of alkyl or methylene groups, further supporting the presence of PE (Du et al. 2022; Wang et al. 2024).

FESEM

FESEM is the most effective technique for magnifying and analyzing surface structures, allowing for the observation of characteristics such as roughness, porosity, and surface cracks (Hussain et al. 2023; Song et al. 2023). As depicted in Fig. 3, PE has an uneven surface composition with elongated chains, prominent valleys, and grooves. This unique surface structure contributes to the expansion of the active site area for adsorption. Guo et al. (2023) validated that the capability of polyethylene microplastics (PE MPs) to adsorb pesticides is attributed to their irregular surfaces (Guo and Wang 2019). The unique characteristics of PE contribute to its superior pollutant adsorption capacity

Fig. 2 FT-IR spectrum of **a** PE, and **b** PE-DZN

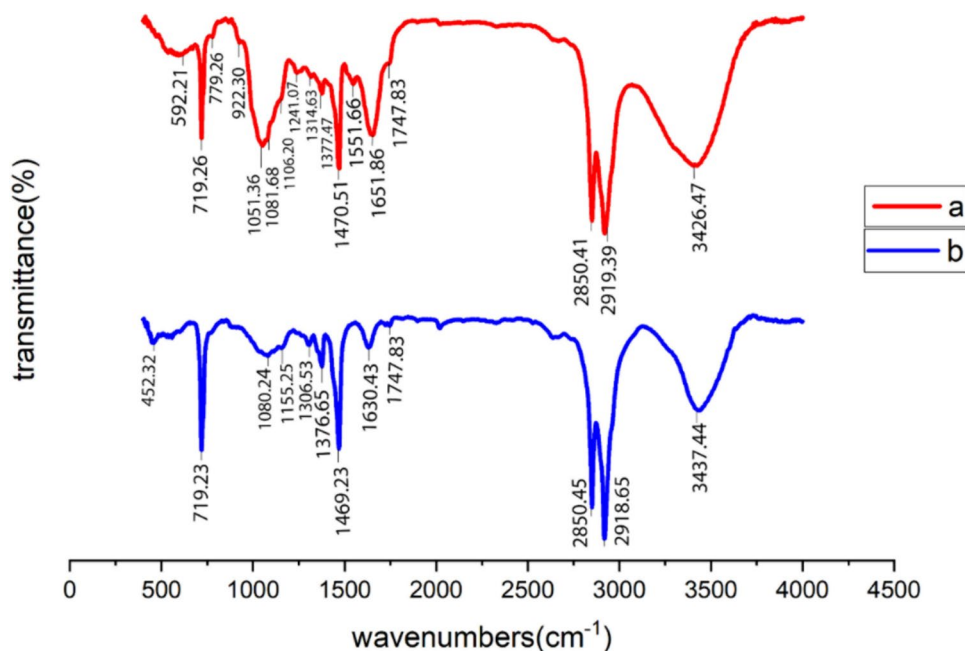
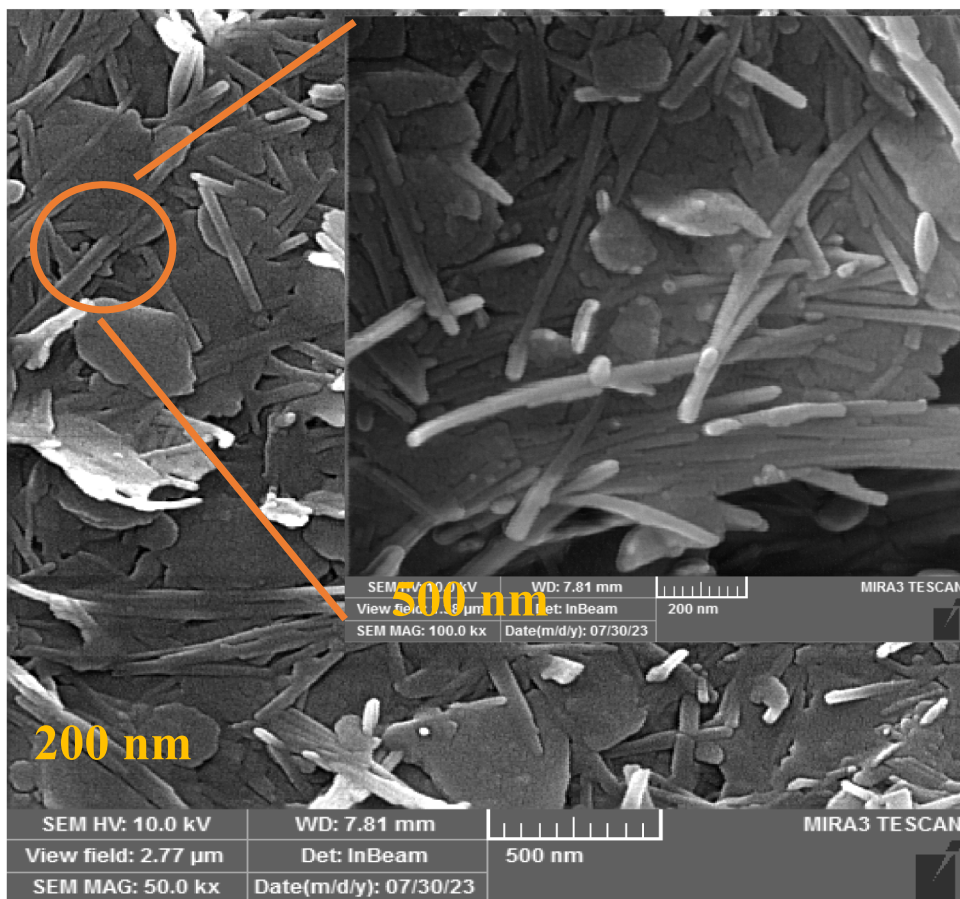


Fig. 3 FESEM images of PE before DZN pesticide adsorption



compared to other types of MPs (Wang et al. 2023a, b). Additionally, the ability of MPs to form strong covalent bonds with pollutants, along with the crystalline structure of PE MPs, enhances their density, mechanical strength, and chemical stability. This makes them an effective carrier for pollutants (Liu et al. 2008; Zhou et al. 2022).

EDX

The EDX analysis was utilized to determine the elemental composition of PE both before and after the adsorption of DZN. Figure 4a and b illustrates the elemental components present in PE prior to and following the adsorption process. As indicated in Fig. 4a, the concentrations of carbon (C), potassium (K), nitrogen (N), oxygen (O), and phosphorus

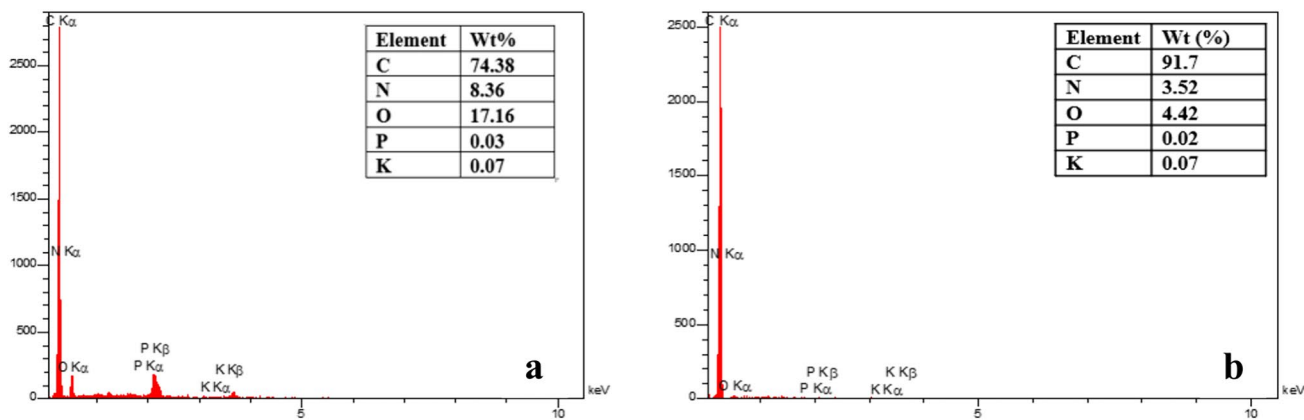


Fig. 4 EDX spectrum of PE **a** before and **b** after DZN adsorption

(P) in PE were 78.38, 0.07, 8.36, 17.16, and 0.03%, respectively. Figure 4b indicates that after the adsorption process, some sulfur (S) and phosphorus (P) atoms from DZN molecules are transferred to the surface of PE, leading to an increased concentration of S and P in PE. The decrease in carbon content may be attributed to the displacement or adsorption of carbon-containing compounds from the surface of PE during the adsorption process. The adsorption of organic compounds, such as DZN, onto MP surfaces can result in changes to the chemical composition of the surface. This process is facilitated by physical adsorption or chemical interactions between the pesticide and the microplastic surface. During the adsorption process, DZN molecules, which contain nitrogen and oxygen, may attach to the surface of PE, leading to an increase in nitrogen and oxygen content (Hadiyanto et al. 2021; Liao et al. 2024a, b).

Mapping analysis

Mapping analysis is used to identify and measure the abundance of elements in the sample (Sobhani et al. 2020). From Fig. 5, the percentage of elements present is indicated by different colors. The highest percentage is related to calcium, carbon, and oxygen elements, while the lowest percentage is related to nitrogen.

ZP

ZP is a measure of the electrostatic dispersion process and the inter-particle stability of desired particles. When coagulating

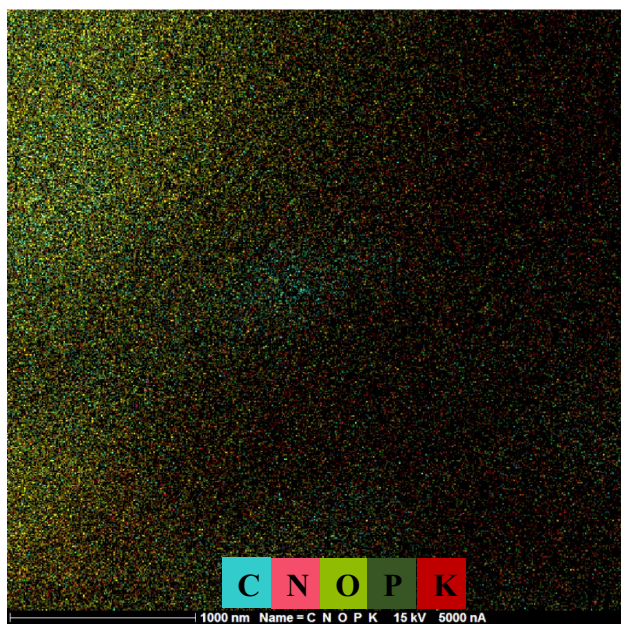


Fig. 5 Map analysis of PE MPs

particles exhibit a substantial positive or negative zeta potential ($\zeta > +30$ mV and $\zeta < -30$ mV), they repel each other, leading to dispersion stability. Conversely, when the zeta potential is close to zero (-30 mV $< \zeta < 30$ mV), there may not be a significant repulsive force to prevent particle aggregation, resulting in dispersion instability (Liao et al. 2024a, b). According to Table 2, the zeta potential value for PE was -36.5 mV.

DLS

DLS is a commonly employed method for assessing the distribution of particle sizes in colloidal suspensions and emulsions. Due to the widely available, easy-to-use, and cost-effective instrumentation, rapid analysis is facilitated (Babick 2020). From Table 2, we used a DLS size of 425 μm for the experiments, because this size was closer to the ambient conditions. Filella (2015) used the microplastic particles at size distribution of ranging from 50 to 425 μm (Filella 2015).

Modeling the DZN adsorption rate

The study examined the impact of various factors, including the amount of PE used, the initial concentration of DZN, contact time, and pH levels, on the adsorption process of DZN. The findings indicate that DZN is effectively adsorbed onto PE.

The experimental results were subjected to statistical analysis employing linear, 2FI, quadratic, and cubic models to ascertain the most suitable model for data representation. From Table 3, the adsorption rate of DZN varied between 18.64 and 98%. Table 4 illustrates the assessment of the statistical validity of the models utilized.

Table 5 displays the coefficients pertaining to the quadratic model (QM) utilized for the adsorption of DZN by PE. As indicated in Table 5, the QM was applied to the empirical data for analysis.

Based on Table 5, the QM for DZN adsorption according to the coded parameters is presented in Eq. (6):

$$\begin{aligned}
 Y = & 75.70 - 7.62A + 8.84B - 7.33C - 3.25D \\
 & + 16.99AB + 4.61AC - 5.87AD \\
 & - 4.68BC + 11.76BD + 7.00CD + 1.17A^2 \\
 & - 4.30B^2 - 37.57C^2 + 11.03D^2
 \end{aligned} \quad (6)$$

In this equation, each model comprises both fixed and variable elements. As per the calculation, the anticipated

Table 2 Zeta potential and DLS values for PE MPs

Material	Zeta potential (mV)	Average diameter (μm)
PE	-36.5	425

Table 3 Matrix of BBD for the adsorption of DZN onto polyethylene

Run No	Coded variable				Removal (%)	Run No	Coded variable				Removal (%)
	A	B	C	D			A	B	C	D	
1	0	0	0	0	73.75	16	1	0	0	1	71.53
2	1	0	1	0	30.75	17	-1	1	0	0	70
3	0	-1	1	0	26.04	18	0	1	-1	0	53.45
4	0	-1	0	1	52.84	19	0	1	1	1	98
5	-1	0	1	0	30.33	20	0	0	0	0	83.45
6	0	0	0	0	77.64	21	0	0	1	1	43.75
7	-1	0	-1	0	54.94	22	0	1	0	-1	86.35
8	0	0	0	0	71.84	23	0	-1	0	-1	88.25
9	1	0	0	-1	93	24	0	0	1	-1	27.64
10	1	0	-1	0	36.93	25	-1	-1	0	0	98
11	1	1	0	0	80.79	26	0	0	-1	1	56.35
12	0	0	-1	-1	68.25	27	0	-1	-1	0	18.64
13	0	0	0	0	71.84	28	-1	0	0	-1	95
14	0	1	1	0	42.15	29	-1	0	0	1	97
15	1	-1	0	0	40.83						

Table 4 Evaluation of statistical adequacy for models

Source	Sequential <i>p</i> value	Lack of Fit <i>p</i> value	Adjusted <i>R</i> ²	Predicted <i>R</i> ²
Linear	0.4339	0.0023	0.0020	0.3212
2FI	0.7751	0.0017	0.1340	1.3077
Quadratic	<0.0001	0.1421	0.8994	0.7344
Cubic	0.0385	0.6707	0.9674	0.8092

Table 5 Coefficients of estimation for the QM of DZN adsorption

Factor	Coefficient Estimate	df	Standard Error	95% CI Low	95% CI High	VIF
Intercept	75.7	1	3.50	68.20	83.21	
A-Conc	-7.62	1	2.26	-12.46	-2.78	1.0000
B-Time	8.84	1	2.26	4.00	13.69	1.0000
C-Dose	-7.33	1	2.26	-12.17	-2.48	1.0000
D-pH	-3.25	1	2.26	-8.10	1.59	1.0000
AB	+16.99	1	3.91	8.60	25.38	1.0000
AC	4.61	1	3.91	-3.78	13.00	1.0000
AD	-5.87	1	3.91	-14.26	2.52	1.0000
BC	-4.68	1	3.91	-13.07	3.72	1.0000
BD	+11.76	1	3.91	3.37	20.16	1.0000
CD	7.00	1	3.91	-1.39	15.39	1.0000
A ²	1.17	1	3.07	-5.42	7.76	1.08
B ²	-4.30	1	3.07	-10.89	2.29	1.08
C ²	-37.57	1	3.07	-44.16	-30.98	1.08
D ²	11.03	1	3.07	4.44	17.62	1.08

adsorption efficiency was determined to be 75.70%. The coded factors A, B, C, and D displayed coefficients of -7.62, +8.84, -7.33, and -3.25, respectively. Factor B had the highest coefficient of +8.84 for the level of DZN adsorption. The variables AB exhibited the most significant interaction effect

with a coefficient of +16.99, whereas the squared effect of D2 emerged as a notable factor with a coefficient of +11.03.

The ANOVA results for the quadratic model are presented in Table 6. The coefficients for *R*², adjusted *R*², predicted *R*², and adequacy precision were calculated as

Table 6 ANOVA for the QM of adsorption rate

	Sum of Squares	Df	Mean Square	F value	P value
Model	16,192.15	14	1156.58	18.89	0.0001
A	696.77	1	696.77	11.38	0.0045
B	939.81	1	939.81	15.33	0.0016
C	643.87	1	643.87	10.52	0.0059
D	126.88	1	126.88	2.07	0.1720
AB	1154.64	1	1154.64	18.86	0.0007
AC	84.92	1	84.92	1.39	0.2586
AD	137.71	1	137.71	2.25	0.1559
BC	87.42	1	87.42	1.43	0.2520
BD	553.66	1	553.66	9.04	0.0094
CD	196.14	1	196.14	3.20	0.0951
A ²	8.86	1	8.86	0.1446	< 0.7094
B ²	120.02	1	120.02	1.96	0.1833
C ²	9154.04	1	9154.04	149.50	0.0001
D ²	788.57	1	788.57	12.88	0.0030
Residual	857.21	14	61.23	—	—
Lack of Fit	759.78	10	75.98	3.12	0.1421
Pure Error	97.43	4	24.36	—	—
Cor Total	17,049.36	28	—	—	—
R ²	0.9497	Predicted R ²	0.7344	—	—
Adjusted R ²	0.8994	Adeq Precision	13.7617	—	—

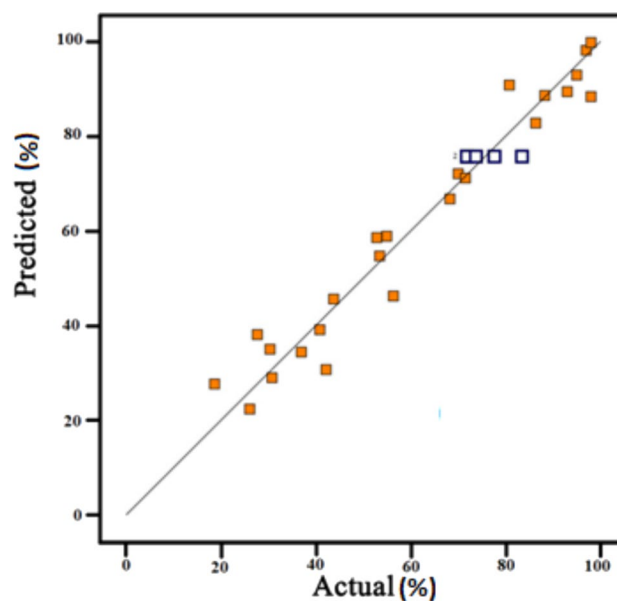
0.94, 0.89, 0.73, and 13.76, respectively. It is important to note that the results outlined in Table 6 were statistically significant (p value < 0.05).

In Table 6, the statistical significance of each primary variable is evidenced by p values below 0.05, indicating a significant impact on the level of DZN adsorption. Furthermore, the difference between R^2 and the expected R^2 is less than 0.2, which aligns with the specified standards for this model. Figure 6 presents a visual representation of the correlation between the observed and projected DZN removal rates. The findings from Fig. 6 indicate proficient performance of the model in accurately forecasting DZN adsorption.

Effect of main factors on adsorption efficiency

Effect of initial DZN concentration

As depicted in Fig. 7a, an increase in concentration from 0.5 to 8.5 mg/L resulted in a 17.85% decrease in adsorption rate. This reduction at higher concentrations is linked to the saturation of active adsorption sites on PE. The binding of DZN molecules to the adsorbent surface may not occur uniformly, leading to reduced efficiency in attaching to the adsorbent surface. Additionally, the presence of specific pesticide

**Fig. 6** Comparison between the experimental and predicted adsorption rates

molecules on the adsorbent creates a repulsive force, which hinders the adsorption of other molecules onto the adsorbent medium (Ren et al. 2024). Zahmatkesh Anbaran et al. (2023) demonstrated that higher initial concentrations result in a decrease in adsorption capacity due to the saturation of active sites on the adsorbent surface (Zahmatkesh Anbarani et al. 2023a, b).

Effect of contact time

According to Fig. 7a, the duration of contact time directly influenced the adsorption of DZN. Consequently, extending the contact time from 10 to 50 min resulted in a 25% increase in adsorption efficiency. Moreover, the optimal contact time for maximum adsorption efficiency was 50 min. With prolonged contact time, there is an increasing likelihood of interaction between DZN pesticide molecules and MPs, leading to a higher adsorption of DZN by polyethylene. Based on the findings, the adsorption of DZN onto PE MPs exhibited a significant increase in the initial stages (Wang et al. 2020a, b). These results were consistent with the study by Li et al. (2021), in which they investigated the adsorption of three pesticides on polyethylene microplastics in aqueous solutions (Li et al. 2021).

Effect of dose

With regard to Fig. 7b, the adsorption rate increased as the adsorbent dosage ranged from 0.2 to 1 g/L and then gradually decreased to approximately 33% (p value < 0.05).

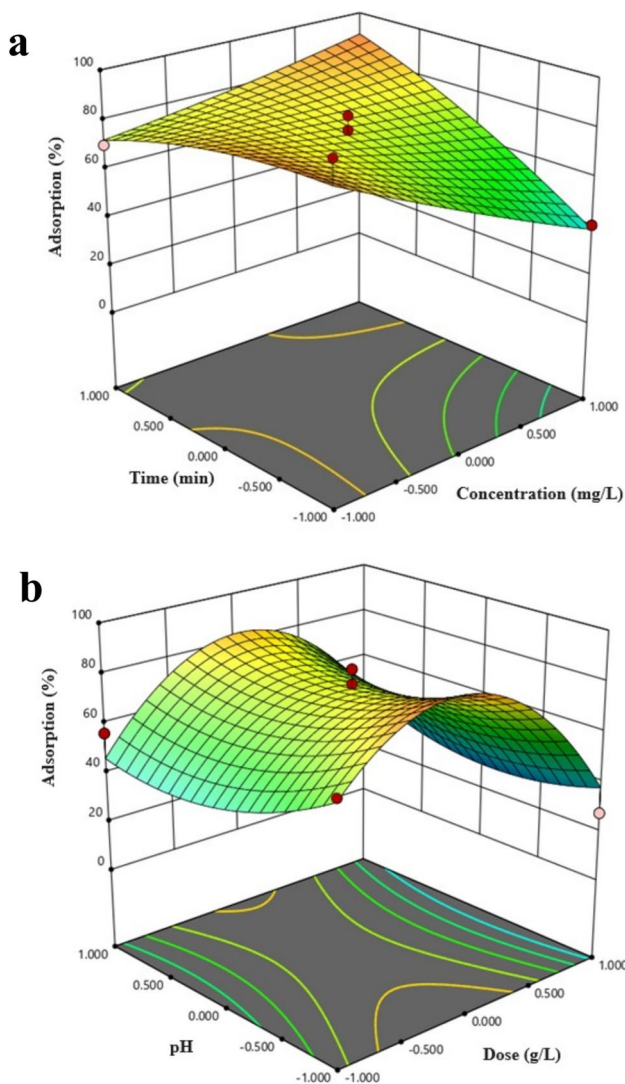


Fig. 7 Response surface plots depicting the effects of time versus concentration (a) and pH versus dose (b)

According to the findings, the optimal dose of adsorbent to achieve the highest adsorption rate of DZN was 0.6 g/L. At high doses, the large quantity of PE particles and their increased proximity to each other hinder the interaction of DZN molecules with all MPs. This reduced the adsorbent-pesticide interaction and slowed down the adsorption process. At low levels of PE, a decrease in the interaction between MPs and the pesticide led to a lower amount of DZN molecules being attached to the surface of PE. Similarly, in a study, it was observed that at low concentrations (ranging from 0.01 to 0.4 g/L), microplastics (MPs) impacted pesticide residues, whereas high concentrations (ranging from 2 to 50 g/L) decreased pesticide residues in water (Wang et al. 2020a, b). In another study, an increase in dosage from 40 to 200 mg/L resulted in a decrease in the adsorption of carbofuran pesticide onto PE from 4.01

to 1.2 mg/g. This suggests a decrease in the availability of unoccupied adsorption sites on the surfaces of MPs (Mo et al. 2021).

Effect of pH

Figure 7b suggests that the rate of DZN adsorption increases at low pH levels, particularly in acidic conditions (p value > 0.05). However, the statistical analysis, with an F value of 2.07 and a p value of 0.1720, indicates that the pH variable does not have a significant impact on the adsorption behavior of DZN. It can be deduced that the surface charge of PE is positive below the isoelectric point and negative above it. The decrease in DZN adsorption onto PE with increasing pH can be attributed to the altered surface properties of PE and the changed chemical behavior of diazinon under different pH conditions. The increased pH might affect the solubility and partitioning behavior of DZN, making it less likely to adhere to the PE surface (Sadeghi et al. 2019). Fang et al. (2019) reported that polystyrene microplastics had the highest adsorption capacity at pH 5.5 for three triazole fungicides, including hexaconazole, myclobutanil, and triadimenol (Fang et al. 2019).

Adsorption isotherms and kinetics

Adsorption isotherms are used to analyze the effectiveness of pollutants' adsorption by investigating the distribution of saturated molecules between liquid and solid phases until equilibrium is achieved (Bonyadi et al. 2023). This research examined the adsorption efficiency of DZN using the Temkin, Langmuir, and Freundlich isotherm models. The kinetic and isotherm parameters for DZN adsorption onto PE are presented in Table 7. According to the Langmuir model, the maximum adsorption capacity of PE for DZN was 0.35 mg/g. From Table 7, the R^2 values for pseudo-first-order kinetics, pseudo-second-order kinetics, and intraparticle diffusion kinetics were 0.91, 0.99, and 0.88, respectively, indicating that adsorption kinetics follows a pseudo-second-order model (Saberzadeh Sarvestani et al. 2016). In a study, it was found that the adsorption of fungicide on PE MPs followed the pseudo-second-order model (Naeimi et al. 2018).

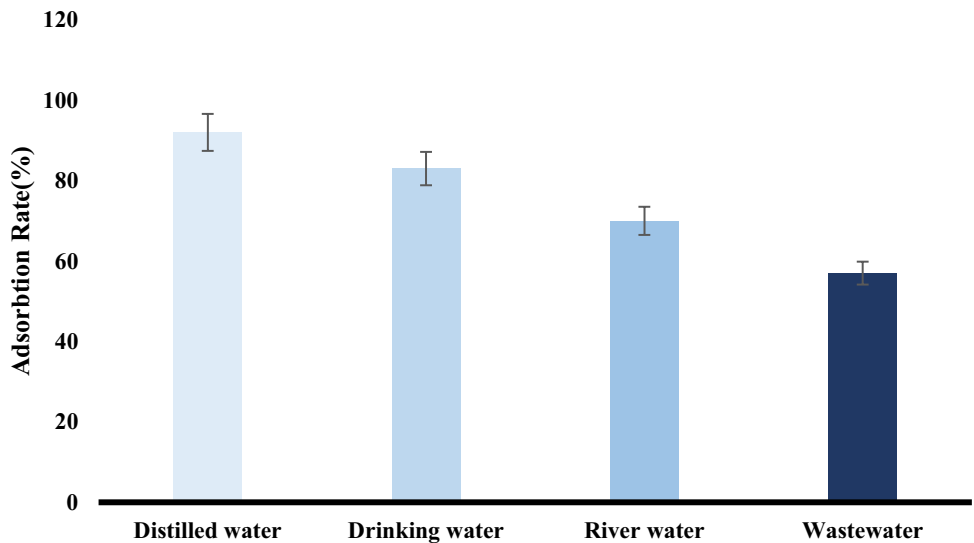
Field studies

Figure 8 illustrates the influence of different water environments on the adsorption of DZN. In this study, samples of distilled water, drinking water, river water, and sewage were used with electrical conductivity (EC) values of 0.001, 0.57, 1.33, and 2.97 mS/cm, respectively. Figure 8 indicates that the highest adsorption rate of DZN (92%) was observed in distilled water, while the lowest adsorption rate (57%) was observed in municipal wastewater. These findings show that

Table 7 Kinetic and isotherm parameters fitted for DZN adsorption

Kinetic model	Linear form	Parameter	Value		
			10 mg.L-1	15 mg.L-1	20 mg.L-1
Pseudo- first order	$\text{Log}(q_e - q_t) = \log q_e - \frac{k_1}{2.303} \cdot t$	q_e, cal [mg/g]	0.9687	1.1251	1.136
		K_1 [min-1]	1.0282	-2.745	1.462
		R^2	0.91	1	0.995
Pseudo- second order	$\frac{t}{q_t} = \frac{1}{k_2 q_e^2} + \frac{1}{q_e} \cdot t$	q_e, cal [mg/g]	7.2046	3.483	3.898
		K^2 [min-1]	-0.020	-1.483	0.1315
		R^2	0.946	0.989	0.99
Intra-particle diffusion	$q_t = k_p \cdot t^{0.5} + c$	K_p [mg/g. min-0.5]	0.3161	0.086	0.356
		R^2	0.97	0.15	0.88
Isotherm model	Linear form	Parameter	Value		
Langmuir	$\frac{C_e}{q_e} = \frac{1}{q_m} C_e + \frac{1}{q_m b}$	$q \text{ max}$ (mg/g)	35.07		
		KL (L/mg)	0.079		
		R^2	0.98		
Freundlich	$\log q_e = \log K_F + \frac{1}{n} \log C_e$	$KF \text{mg/g(L/mg)}^{1/n}$	0.2239		
		n	0.8395		
		R^2	0.7		
Temkin	$q_e = B_1 \ln k_t + B_1 \ln C_e$	$k t$ (L/mg)	0.0019		
		B_1	4.27		
		R^2	0.71		

Fig. 8 Effect of different water resource on DZN adsorption



the presence of ions in aqueous environments has an inhibitory effect, reducing the adsorption rate of DZN (Miranda et al. 2023).

Adsorption thermodynamics

From Table 8, the negative enthalpy (ΔH°) value was determined to be -0.16 kJ/mol , indicating that the adsorption mechanism is exothermic and physical. Therefore, DZN molecules adhere to polyethylene particles due to van der

Table 8 Thermodynamics parameters for DZN adsorption onto PE

T ($^\circ\text{K}$)	$\text{Ln } k$	ΔG° (kJ/mol)	ΔH° (kJ/mol)	Δi° (J/(mol K))
288	0.0229	-55.011	-0.16	54.41
298	0.0170	-42.19		
308	0.0110	-28.36		
318	0.0068	-18.03		

Waals forces. This force facilitates the dispersion of DZN molecules throughout the absorbent material without being confined to a specific location (Ohale et al. 2023). The positive value of entropy (ΔS°) of 54.41 J/(mol K) indicates that the system is becoming more disordered, while a negative value of Gibbs free energy (ΔG°) indicates a spontaneous and thermodynamically favorable process. Therefore, it can be concluded that the adsorption of DZN onto PE MPs is an exothermic, highly disordered, and spontaneous process (Jiménez-Skrzypek et al. 2021).

Effect of different ions

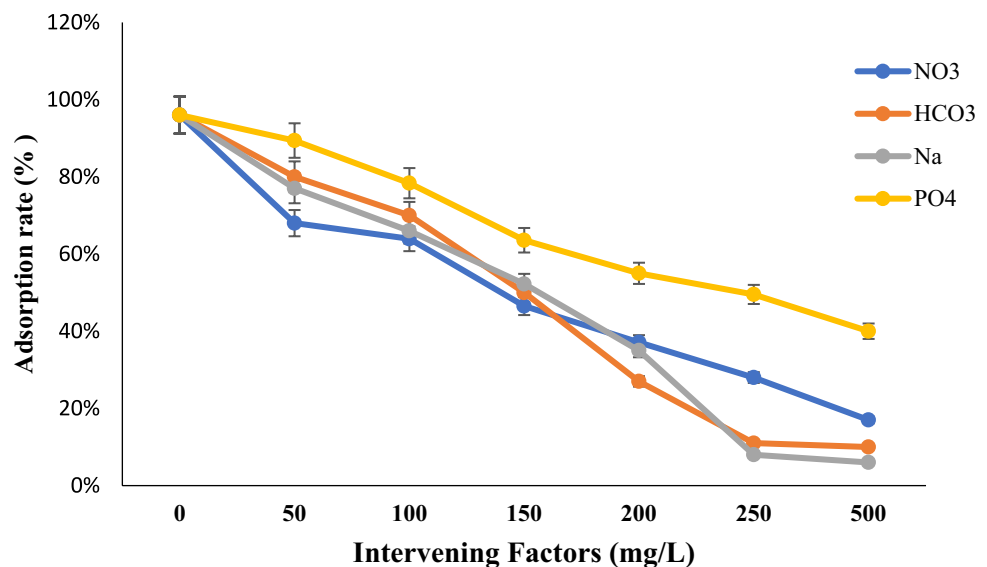
In this research, the study focused on investigating the influence of interfering compounds on the adsorption rate of DZN. The study specifically focused on investigating the influence of substances such as NaHCO_3 , NaNO_3 , Na_2HPO_4 , and NaCl on the adsorption rate of DZN. Figure 9 illustrates the adsorption rate under varying concentrations of these ions, ranging from 50 to 500 mg/L. The findings indicate a reduction in the adsorption rate of DZN as the concentrations of interfering compounds increase (Ren et al. 2020). Phosphate ions significantly reduce the rate of DZN adsorption, leading to a complete absence of adsorption. Phosphate and sodium ions compete with larger contaminants, such as DZN molecules, for adsorption onto the surface of PE. As a result, these ions are adsorbed more quickly than DZN, which reduces the efficacy of the DZN adsorption process. In addition, anions such as HCO_3^- and NO_3^- can form hydrophobic complexes with DZN, thereby reducing its adsorption capacity. NaCl , being a common compound in aquatic environments, significantly affects the adsorption of pesticides onto MPs. As the salinity increases, Na^+ cations readily attach to negatively charged MPs through

electrostatic interactions, hindering the adsorption of DZN onto MPs (Fang et al. 2019). Furthermore, the addition of NaCl to the solution leads to an increase in H^+ ion concentration, which in turn decreases the adsorption efficiency (Wang et al. 2020a, b). Wang et al. (2020a, b) indicated that the presence of Na^+ reduced the solubility of pesticides in aqueous solution and promoted the adsorption of pesticides on hydrophobic PE MPs (Wang et al. 2020a, b). Similarly, the adsorption capacity of sulfamethazine on PE, PVC, and PP decreases with increasing salinity due to electrostatic interactions, which is consistent with our findings (Liang et al. 2023). In a study, it was found that higher salinity levels led to a decrease in pesticide adsorption on PE (Jiang et al. 2020).

Conclusion

In this study, BBD was used to investigate the adsorption of DZN pesticide on PE MPs. The highest adsorption efficiency (98%) was attained at pH 7, a 10-min contact time, an adsorbent dosage of 0.6 g/L, and a DZN concentration of 0.5 mg/L. The findings followed the pseudo-second-order model and the Langmuir isotherm model. DZN molecules were adsorbed onto PE through intermolecular interactions and covalent bonding. According to the Langmuir model, the maximum adsorption capacity of PE for DZN was 0.35 mg/g. The results indicated that the highest adsorption rate of DZN (92%) was observed in distilled water, while the lowest adsorption rate (57%) was observed in municipal wastewater. The ΔH° and ΔS° values were obtained as -0.16 kJ/mol and 54.41 J/(mol K), respectively. Therefore, regarding negative ΔG° values, it can be concluded that the adsorption of DZN onto PE MPs is an exothermic, highly

Fig. 9 Impact of various ions on DZN adsorption



disordered, and spontaneous process. The findings indicate a reduction in the adsorption rate of DZN as the concentrations of interfering compounds increase. This research offers valuable insights into the primary mechanisms and variables influencing the environmental fate of pesticides and MPs, which are crucial for managing and evaluating associated risks in aquatic ecosystems.

Authors' contributions MY performed the experiments and wrote the paper; ZB wrote and edited the paper, and conceived and designed the experiments; AN designed the experiments; BB analyzed data.

Funding The authors would like to thank the financial support provided by the Mashhad University of Medical Sciences (Iran) through the grant number of 4001565.

Data availability All necessary data are included in the document.

Declarations

Conflict of interest The authors declare that they have no conflict of interests.

Ethical approval This article does not contain any studies with human participants or animals performed by any of the authors.

Open Access This article is licensed under a Creative Commons Attribution 4.0 International License, which permits use, sharing, adaptation, distribution and reproduction in any medium or format, as long as you give appropriate credit to the original author(s) and the source, provide a link to the Creative Commons licence, and indicate if changes were made. The images or other third party material in this article are included in the article's Creative Commons licence, unless indicated otherwise in a credit line to the material. If material is not included in the article's Creative Commons licence and your intended use is not permitted by statutory regulation or exceeds the permitted use, you will need to obtain permission directly from the copyright holder. To view a copy of this licence, visit <http://creativecommons.org/licenses/by/4.0/>.

References

- Babick F (2020) Chapter 3.2.1—Dynamic light scattering (DLS). In: Hodoroba V-D, Unger WES, Shard AG (eds) Characterization of nanoparticles. Elsevier, Amsterdam, pp 137–172
- Bai B, Bai F, Nie Q, Jia X (2023) A high-strength red mud-fly ash geopolymer and the implications of curing temperature. *Powder Technol* 416:118242
- Barari F, Bonyadi Z (2023) Evaluation of the leaching of microplastics from discarded medical masks in aquatic environments: a case study of Mashhad city. *Appl Water Sci* 13:229
- Beg M, Kormin S, Bijarimi M, Zaman HU (2016) Preparation and characterization of low-density polyethylene/thermoplastic starch composites. *Adv Polym Technol*. <https://doi.org/10.1002/adv.21521>
- Bonyadi Z, Dehghan A, Sadeghi A (2012) Determination of sonochemical technology efficiency for cyanide removal from aqueous solutions. *World Appl Sci J* 18:425–429
- Bonyadi Z, Khatibi FS, Alipour F (2022) Ultrasonic-assisted synthesis of Fe₃O₄ nanoparticles-loaded sawdust carbon for malachite green removal from aquatic solutions. *Appl Water Sci* 12:221
- Bonyadi Z, Fouladi Z, Robotjazi A, Zahmatkesh Anbarani M (2023) Reactive red-141 removal from synthetic solutions by γ -Al₂O₃ nanoparticles: process modeling, kinetic, and isotherm studies. *Appl Water Sci* 13:52
- Caro E, Comas E (2017) Polyethylene comonomer characterization by using FTIR and a multivariate classification technique. *Talanta* 163:48–53
- Chen J, Bai B, Du Q (2024) Durability evaluation of a high-performance red mud-based composite material. *Mater Today Commun* 39:108684
- Cheng Z, Hou Z, Han H, Yu X, Li J, Zhao Q, Zhang N, Lu Z (2023) Adsorption, mobility, and degradation of the pesticide propaquizafop in five agricultural soils in China. *Sci Rep* 13:5814
- Du H, Zhang Y, Jiang H, Wang H (2022) Adsorption of rhodamine B on polyvinyl chloride, polystyrene, and polyethylene terephthalate microplastics in aqueous environments. *Environ Technol Innov* 27:102495
- Ehrampoush MH, Sadeghi A, Ghaneian MT, Bonyadi Z (2017) Optimization of diazinon biodegradation from aqueous solutions by *Saccharomyces cerevisiae* using response surface methodology. *AMB Express* 7:1–6
- Esmaili Nasrabadi A, Zahmatkesh Anbarani M, Bonyadi Z (2023) Investigating the efficiency of oak powder as a new natural coagulant for eliminating polystyrene microplastics from aqueous solutions. *Sci Rep* 13:20402
- Esmaili Z, Barikbin B, Shams M, Alidadi H, Al-Musawi TJ, Bonyadi Z (2023) Biosorption of metronidazole using *Spirulina platensis* microalgae: process modeling, kinetic, thermodynamic, and isotherm studies. *Appl Water Sci* 13:63
- Eydi Gabrabad M, Yari M, Bonyadi Z (2024) Using *Spirulina platensis* as a natural biocoagulant for polystyrene removal from aqueous medium: performance, optimization, and modeling. *Sci Rep* 14:2506
- Fang S, Yu W, Li C, Liu Y, Qiu J, Kong F (2019) Adsorption behavior of three triazole fungicides on polystyrene microplastics. *Sci Total Environ* 691:1119–1126
- Filella M (2015) Questions of size and numbers in environmental research on microplastics: methodological and conceptual aspects. *Environ Chem* 12:527–538
- Foroutan R, Mohammadi R, Sohrabi N, Sahebi S, Farjadfar S, Esvandi Z, Ramavandi B (2020) Calcined alluvium of agricultural streams as a recyclable and cleaning tool for cationic dye removal from aqueous media. *Environ Technol Innov* 17:100530
- Frescura LM, Funari Junior RA, Brummelhaus de Menezes B, de Moraes F, Bastos A, Barcellos da Rosa M (2023) Interaction of fluorene and its analogs with high-density polyethylene microplastics: an assessment of the adsorption mechanism to establish the effects of heteroatoms in the molecule. *Environ Pollut* 337:122573
- Guo X, Wang J (2019) Sorption of antibiotics onto aged microplastics in freshwater and seawater. *Marine Pollut Bull* 149:110511
- Hadiyanto H, Khoironi A, Dianratri I, Suherman S, Muhammad F, Vaidyanathan S (2021) Interactions between polyethylene and polypropylene microplastics and *Spirulina* sp. microalgae in aquatic systems. *Heliyon* 7:e07676
- Haji Abolhasani M, Sahebghadam Lotfi A (2022) Performance evaluation of soil microorganism producing organophosphate hydrolase enzyme in detoxification of organophosphorus compounds (diazinon) and its kinetic properties assessment. *Cell Mol Res (iran J Biol)* 35:60–74
- Hussain S, Shah ZA, Sabiruddin K, Keshri AK (2023) Characterization and tribological behavior of Indian clam seashell-derived hydroxyapatite coating applied on titanium alloy by plasma spray technique. *J Mech Behav Biomed Mater* 137:105550
- Jiang M, Hu L, Lu A, Liang G, Lin Z, Zhang T, Xu L, Li B, Gong W (2020) Strong sorption of two fungicides onto biodegradable

- microplastics with emphasis on the negligible role of environmental factors. *Environ Pollut* 267:115496
- Jiménez-Skrzypek G, Ortega-Zamora C, González-Sálamo J, Hernández-Sánchez C, Hernández-Borges J (2021) The current role of chromatography in microplastic research: plastics chemical characterization and sorption of contaminants. *J Chromatogr Open* 1:100001
- Kafaei R, Arfaeinia H, Savari A, Mahmoodi M, Rezaei M, Rayani M, Sorial GA, Fattahi N, Ramavandi B (2020) Organochlorine pesticides contamination in agricultural soils of southern Iran. *Chemosphere* 240:124983
- Lan T, Wang T, Cao F, Yu C, Chu Q, Wang F (2021) A comparative study on the adsorption behavior of pesticides by pristine and aged microplastics from agricultural polyethylene soil films. *Ecotox Environ Saf* 209:111781
- Li H, Wang F, Li J, Deng S, Zhang S (2021) Adsorption of three pesticides on polyethylene microplastics in aqueous solutions: Kinetics, isotherms, thermodynamics, and molecular dynamics simulation. *Chemosphere* 264:128556
- Liang Y, Ying C, Zhu J, Zhou Q, Sun K, Tian Y, Li J (2023) Effects of salinity, pH, and Cu(II) on the adsorption behaviors of tetracycline onto polyvinyl chloride microplastics: a site energy distribution analysis. *Water*. <https://doi.org/10.3390/w15101925>
- Liao H, Su J, Han J, Xiao T, Sun X, Cui G, Duan X, Shi P (2024a) An intrinsic self-healable, anti-freezable and ionically conductive hydrogel for soft ionotronics induced by imidazolyl cross-linker molecules anchored with dynamic disulfide bonds. *Macromol Rapid Commun* 45:2300613
- Liao H, Zhong W, Li C, Han J, Sun X, Xia X, Li T, Noori A, Mousavi MF, Liu X (2024b) An intrinsically self-healing and anti-freezing molecular chains induced polyacrylamide-based hydrogel electrolytes for zinc manganese dioxide batteries. *J Energy Chem* 89:565–578
- Liu W, Huang F, Liao Y, Zhang J, Ren G, Zhuang Z, Zhen J, Lin Z, Wang C (2008) Treatment of CrVI-containing Mg(OH)₂ nano-waste. *Angew Chem* 120:5701–5704
- Miranda MN, Fernandes ART, Silva AMT, Pereira MFR (2023) Behavior and removal of microplastics during desalination in a lab-scale direct contact membrane distillation system. *Desalination* 565:116846
- Mo Q, Yang X, Wang J, Xu H, Li W, Fan Q, Gao S, Yang W, Gao C, Liao D, Li Y, Zhang Y (2021) Adsorption mechanism of two pesticides on polyethylene and polypropylene microplastics: DFT calculations and particle size effects. *Environ Pollut* 291:118120
- Mongil-Manso J, Jiménez-Ballesta R, Trujillo-González JM, San José Wery A, Díez Méndez A (2023) A comprehensive review of plastics in agricultural soils: a case study of Castilla y León (Spain) farmlands. *Land* 12:1888
- Naeimi B, Foroutan R, Ahmadi B, Sadeghzadeh F, Ramavandi B (2018) Pb(II) and Cd(II) removal from aqueous solution, shipyard wastewater, and landfill leachate by modified *Rhizopus oryzae* biomass. *Mater Res Express* 5:045501
- Nasrabadi AE, Eydi M, Bonyadi Z (2023) Utilizing *Chlorella vulgaris* algae as an eco-friendly coagulant for efficient removal of polyethylene microplastics from aquatic environments. *Heliyon* 9:e22338
- Ohale PE, Igwegbe CA, Iwuozor KO, Emenike EC, Obi CC, Białowiec A (2023) A review of the adsorption method for norfloxacin reduction from aqueous media. *MethodsX* 10:102180
- Pirsaheb M, Khodadadi T, Bonyadi Z, Sharafi K, Khosravi T (2013) Evaluation of pesticide residues 2, 4-D, Atrazine and Alachlor concentration in drinking water well of Mahidasht district-Kermanshah, Iran, 2010–2011. *World Appl Sci J* 23:1530–1537
- Ren W, Zhou P, Nie G, Cheng C, Duan X, Zhang H, Wang S (2020) Hydroxyl radical dominated elimination of plasticizers by peroxymonosulfate on metal-free boron: kinetics and mechanisms. *Water Res* 186:116361
- Ren S, Xu X, Zhu Z-S, Yang Y, Tian W, Hu K, Zhong S, Yi J, Duan X, Wang S (2024) Catalytic transformation of microplastics to functional carbon for catalytic peroxymonosulfate activation: conversion mechanism and defect of scavenging. *Appl Catal B Environ* 342:123410
- Saberzadeh Sarvestani F, Esmaeili H, Ramavandi B (2016) Modification of *Sargassum angustifolium* by molybdate during a facile cultivation for high-rate phosphate removal from wastewater: structural characterization and adsorptive behavior. *3 Biotech* 6:251
- Sadeghi A, Ehrampoush MH, Ghaneian MT, Najafpoor AA, Fallahzadeh H, Bonyadi Z (2019) The effect of diazinon on the removal of carmoisine by *Saccharomyces cerevisiae*. *Desalin Water Treat* 137:273–278
- Salama K, Geyer M (2023) Plastic mulch films in agriculture: their use, environmental problems. *Recycl Altern Environ* 10:179
- Sobhani Z, Zhang X, Gibson C, Naidu R, Megharaj M, Fang C (2020) Identification and visualization of microplastics/nanoplastics by Raman imaging (i): down to 100 nm. *Water Res* 174:115658
- Song Z, Han D, Yang M, Huang J, Shao X, Li H (2023) Formic acid formation via direct hydration reaction (CO + H₂O → HCOOH) on magnesia-silver composite. *Appl Surf Sci* 607:155067
- Wang F, Gao J, Zhai W, Liu D, Zhou Z, Wang P (2020a) The influence of polyethylene microplastics on pesticide residue and degradation in the aquatic environment. *J Hazard Mater* 394:122517
- Wang T, Yu C, Chu Q, Wang F, Lan T, Wang J (2020b) Adsorption behavior and mechanism of five pesticides on microplastics from agricultural polyethylene films. *Chemosphere* 244:125491
- Wang L, Yang H, Guo M, Wang Z, Zheng X (2023a) Adsorption of antibiotics on different microplastics (MPs): behavior and mechanism. *Sci Total Environ* 863:161022
- Wang Y-N, Wang Q, Li Y, Wang H, Gao Y, Sun Y, Wang B, Bian R, Li W, Zhan M (2023b) Impact of incineration slag co-disposed with municipal solid waste on methane production and methanogens ecology in landfills. *Bioresour Technol* 377:128978
- Wang Z, Fernández-Blanco C, Chen J, Veiga MC, Kennes C (2024) Effect of electron acceptors on product selectivity and carbon flux in carbon chain elongation with *Megasphaera hexanoica*. *Sci Total Environ* 912:169509
- Yu Z, Xu X, Guo L, Yuzuak S, Lu Y (2024) Physiological and biochemical effects of polystyrene micro/nano plastics on *Arabidopsis thaliana*. *J Hazard Mater* 469:133861
- Zafarzadeh A, Taghani JM, Toomaj MA, Ramavandi B, Bonyadi Z, Sillanpää M (2021) Assessment of the health risk and geo-accumulation of toxic metals in agricultural soil and wheat, northern Iran. *Environ Monit Assess* 193:1–10
- Zahmatkesh Anbarani M, Esmaeili Nasrabadi A, Bonyadi Z (2023a) Use of *Saccharomyces cerevisiae* as a new technique to remove polystyrene from aqueous medium: modeling, optimization, and performance. *Appl Water Sci* 13:166
- Zahmatkesh Anbarani M, Najafpoor A, Barikbin B, Bonyadi Z (2023b) Adsorption of tetracycline on polyvinyl chloride microplastics in aqueous environments. *Sci Rep* 13:17989
- Zahmatkesh Anbarani M, Esmaeili Nasrabadi A, Bonyadi Z (2024) Aging effect on the adsorption behavior of microfibers obtained from cigarette butts in aqueous solutions. *Appl Water Sci* 14:30
- Zhang C, Lei Y, Qian J, Qiao Y, Liu J, Li S, Dai L, Sun K, Guo H, Sui G (2021) Sorption of organochlorine pesticides on polyethylene microplastics in soil suspension. *Ecotox Environ Saf* 223:112591
- Zhou D, Luo H, Zhang F, Wu J, Yang J, Wang H (2022) Efficient photocatalytic degradation of the persistent PET fiber-based microplastics over Pt nanoparticles decorated N-doped TiO₂ nanoflowers. *Adv Fiber Mater* 4:1094–1107
- Zhou R, Bai B, Cai G, Chen X (2024) Thermo-hydro-mechanical coupling model for hydrate-bearing sediment within a unified granular thermodynamic theory. *Comput Geotech* 167:106057